

LETTER • OPEN ACCESS

## Deciphering the relationship between vegetation and Indian summer monsoon rainfall

To cite this article: Jerry B Samuel *et al* 2023 *Environ. Res. Lett.* **18** 044023

View the [article online](#) for updates and enhancements.

### You may also like

- [What influences climate and glacier change in southwestern China?](#)  
Tepppei J Yasunari
- [Changes in snow cover over China in the 21st century as simulated by a high resolution regional climate model](#)  
Ying Shi, Xuejie Gao, Jia Wu et al.
- [Spatiotemporal changes of green cover pattern in urban areas of Batticaloa, Sri Lanka](#)  
M Seevarethnam, V Selvanayagam and N Rusli

ENVIRONMENTAL RESEARCH  
LETTERS

## LETTER

## Deciphering the relationship between vegetation and Indian summer monsoon rainfall

## OPEN ACCESS

## RECEIVED

12 December 2022

## REVISED

25 February 2023

## ACCEPTED FOR PUBLICATION




8 March 2023

## PUBLISHED

31 March 2023

Original Content from this work may be used under the terms of the [Creative Commons Attribution 4.0 licence](#).

Any further distribution of this work must maintain attribution to the author(s) and the title of the work, journal citation and DOI.

Jerry B Samuel<sup>1,2,\*</sup> , Arindam Chakraborty<sup>1,2,3</sup>  and Anagha Paleri<sup>4</sup> <sup>1</sup> Centre for Atmospheric and Oceanic Sciences, Indian Institute of Science, Bengaluru, Karnataka 560012, India<sup>2</sup> Divecha Centre for Climate Change, Indian Institute of Science, Bengaluru, Karnataka 560012, India<sup>3</sup> DST-Centre of Excellence in Climate Change, Divecha Centre for Climate Change, Indian Institute of Science, Bengaluru, Karnataka 560012, India<sup>4</sup> Climate Connect Digital, Pune, India

\* Author to whom any correspondence should be addressed.

E-mail: [jerrysamuel@iisc.ac.in](mailto:jerrysamuel@iisc.ac.in)**Keywords:** vegetation, monsoon, stabilitySupplementary material for this article is available [online](#)**Abstract**

Land surface utilization in the Indian subcontinent has undergone dramatic transformations over the years, altering the region's surface energy flux partitioning. The resulting changes in moisture availability and atmospheric stability can be critical in determining the season's monsoon rainfall. This study uses fully coupled global climate model simulations with idealized land cover to elucidate the consequences of land surface alterations. We find that an increase in forest cover, in general, increases precipitation in India. However, precipitation is not a linear function of forest-covered-area due to the spatially heterogeneous nature of the impact. A fully forest-covered India receives less precipitation than when the forest covers only the eastern side of India, occupying just about half the area. This signifies the importance of the east-west gradient in vegetation cover observed over India. Using an energy balance model, we diagnose that the diverse nature of this precipitation response results from three different pathways: evaporation from the surface, the net energy input into the atmosphere, and moist stability. Evaporation exhibits a linear relationship with forest-covered-area and reveals minimal spatial heterogeneity. On the contrary, the influence through the other two pathways is found to be region specific. Rainfall modulation via changes in net energy input is dominant in the head Bay of Bengal region, which is susceptible to convective systems. Whereas impact through stability changes is particularly significant south of 20° N. In addition, we find that moisture advection modulates the significance of these pathways over northwest India. Thus, the impact of land cover changes act via three effective mechanisms and are region dependent. The findings in this study have broader ramifications since the dominant region-specific mechanisms identified are expected to be valid for other forcings and are not just limited to the scenarios considered here.

**1. Introduction**

Zonal mean meridional circulation in the tropics is dominated by the cross-equatorial Hadley cell, the ascending branch of which colocates with a band of deep convective clouds, forming the intertropical convergence zone (ITCZ), which is a region of precipitation maxima and energy flux divergence (Kang *et al* 2008, Donohoe *et al* 2013). Although these systems have been studied as part of the zonal mean meridional overturning circulation using the energy budget

framework, considerable challenges exist when the zonal asymmetries are taken into account (Biasutti *et al* 2018). These heterogeneities arising out of land surface variabilities, land-sea contrasts, aerosol concentrations, and influence of orography define the intricate characteristics of regional monsoon systems (Wang *et al* 2017).

Monsoons are large-scale precipitating systems that have a prominent role in interhemispheric atmospheric energy transport (Schneider *et al* 2014, Boos and Korty 2016). The seasonal transition of the ITCZ

is found to be associated with the cross-equatorial atmospheric energy transport and the local equatorial net energy input into the atmosphere (Adam *et al* 2016). Along with net energy input, moist stability also plays a significant role in low-level convergence in the tropics (Neelin and Held 1987). Large-scale tropical precipitation, which colocalizes with the regions of convergence, is also determined to a first-order by the net energy input and moist stability along with surface evaporation (Srinivasan 2001, 2003). Precipitation estimate from this energetics framework agrees well with observed values at seasonal, and paleo timescales (Srinivasan 2001, Jalihal *et al* 2019). Although the spatiotemporal variability of the monsoon is influenced by various remote and local forcings such as the El-Niño Southern Oscillation, Eurasian snow cover, aerosols, and land surface processes (Joseph *et al* 1994, Meehl 1994, Webster *et al* 1998, Bamzai and Shukla 1999, Ramanathan *et al* 2005), these forcings could be influencing the seasonal monsoon precipitation via the same basic pathways, namely the energy input, moisture availability and moist stability in the region. A unified framework connecting these diverse forcings with monsoon variability would be of great practical importance. It can also be hypothesized that these pathways exhibit regional preferences. The energetics approach can be employed to understand this spatial heterogeneity and the relative importance of the various pathways. Since land cover influences surface energy partitioning and moisture availability, land cover changes can be used to study the significance of the various pathways.

The land surface is known to modulate the spatiotemporal variability of monsoon, by influencing the propagation of onset isochrones (Krishnamurti *et al* 2012), modulating intra-seasonal oscillations (Saha *et al* 2012), and affecting the withdrawal of the monsoon (Pathak *et al* 2014). Several previous studies have stressed the significance of hydrological processes on monsoon (Webster 1983, Asharaf *et al* 2012, Agrawal and Chakraborty 2016). Vegetation cover exerts tremendous influence on the hydrological processes over land (Bonan 2008). Zhang *et al* (2021, 2022) have demonstrated that increasing the vegetation cover in the Loess Plateau in China leads to net increase in water yield. Chakraborty *et al* (2023) has shown that vegetation changes influence monsoon onset predictions by modulating moisture advection over Indian land. Further, Indian monsoon rainfall has declined due to the reduction in forest cover (Devaraju *et al* 2015, Paul *et al* 2016). On a global scale, deforestation can lead to spatially heterogeneous impacts with tropical warming and high latitude cooling (Lee *et al* 2011, Duveiller *et al* 2018). It is plausible that such spatial variability exists at regional scales as well. Since forest cover impacts the climate via various radiative and nonradiative processes (Davin and Noblet-Ducoudre

2010), influencing both surface temperature and precipitation, the energetics approach can be used to investigate the different mechanisms determining the vegetation-climate dynamics.

In this study, we explore the mechanisms/pathways linking forest cover to precipitation, and their spatial distribution.

## 2. Model details and experiments

Climate Forecast System version-2 (CFSv2), an atmosphere-land-ocean coupled dynamical forecast system is used to perform the experiments. The atmospheric component in CFSv2 is the Global Forecast System model. The spectral triangular truncation used in our experiments is 126 waves (about  $0.9375^\circ$  horizontal resolution). The model has 64 hybrid sigma-pressure levels. The ocean model in CFSv2 is the Geophysical Fluid Dynamics Laboratory Modular Ocean Model v4 (GFDL MOM4) with  $0.25^\circ$  horizontal resolution in the equatorial region ( $\pm 10^\circ$  latitude) and  $0.5^\circ$  elsewhere. Land surface processes are represented by the NOAH land surface model. Saha *et al* (2014) gives a detailed description of the CFSv2 model. The version of CFSv2 employed here is similar to that used in Rajendran *et al* (2021) and Chakraborty *et al* (2023).

Four simplistic and carefully-designed experiments using the CFSv2 are performed to explore the objectives of this study. The first experiment, termed BSL (figure 1(b)), consists of making the entire Indian region devoid of vegetation by specifying the CFSv2 vegetation class, bare soil, over the region. In the second experiment, termed TRF (figure 1(a)), the entire Indian region is covered by the vegetation class tropical rainforest. These two experiments represent two drastically distinct vegetation regimes which would help highlight the impact of land surface changes on monsoon. The absence of spatial heterogeneity in land surface vegetation over the Indian region also makes it less cumbersome to delineate the physical mechanisms involved. Further, this helps to identify the spatial heterogeneity in the response to a uniform vegetation change. We performed two more experiments to bring out the impact of spatially varying vegetation patterns. EXP1 (figure 1(c)) is designed such that tropical rainforest covers the western side of India while the eastern side has bare soil. This experiment helps understand the effect of increasing the forest cover over the generally arid northwest India. Here, we try to answer whether the increased evaporation enhances rainfall over these regions. In contrast, in EXP2 (figure 1(d)), the eastern side of India has tropical rainforest cover while the western side has bare soil, reminiscent of the east-west asymmetry in aridity over India (see supplementary text for a discussion). Compared to TRF, this vegetation pattern could increase the east-west evaporation gradient. Since the fraction of land

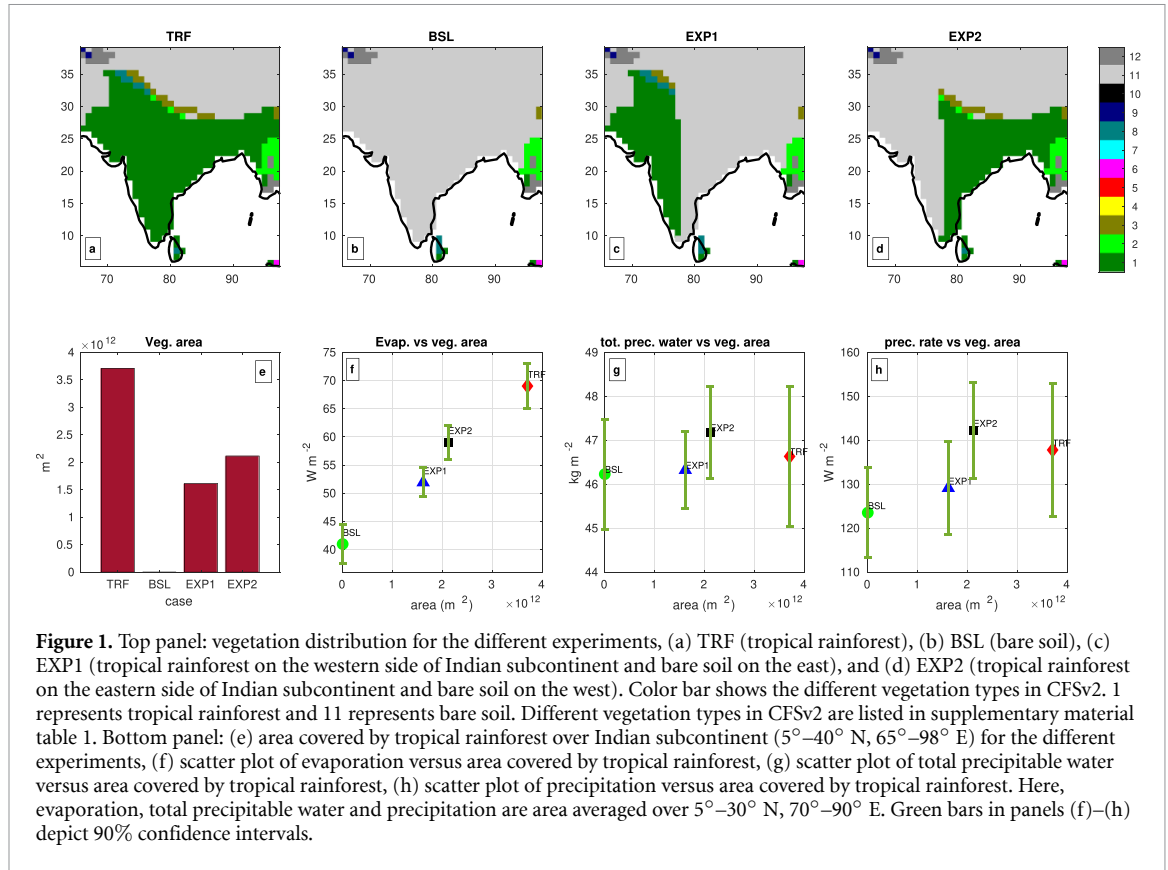


**Figure 1.** Top panel: vegetation distribution for the different experiments, (a) TRF (tropical rainforest), (b) BSL (bare soil), (c) EXP1 (tropical rainforest on the western side of Indian subcontinent and bare soil on the east), and (d) EXP2 (tropical rainforest on the eastern side of Indian subcontinent and bare soil on the west). Color bar shows the different vegetation types in CFSv2. 1 represents tropical rainforest and 11 represents bare soil. Different vegetation types in CFSv2 are listed in supplementary material table 1. Bottom panel: (e) area covered by tropical rainforest over Indian subcontinent (5°–40° N, 65°–98° E) for the different experiments, (f) scatter plot of evaporation versus area covered by tropical rainforest, (g) scatter plot of total precipitable water versus area covered by tropical rainforest, (h) scatter plot of precipitation versus area covered by tropical rainforest. Here, evaporation, total precipitable water and precipitation are area averaged over 5°–30° N, 70°–90° E. Green bars in panels (f)–(h) depict 90% confidence intervals.

covered by vegetation is a function of its type and season, the existing monthly vegetation fraction over locations of modified vegetation type is replaced with a representative seasonal cycle. In all these cases, the CFSv2 model was run starting 00 GMT of 20 May up to 30 September for the years 2011–2020 (except for 2017 due to the unavailability of compatible initial conditions). The initial conditions were taken from National Centers for Environmental Information ([www.ncei.noaa.gov/data/climate-forecast-system/access/operational-analysis/initial-conditions-high-resolution/](http://www.ncei.noaa.gov/data/climate-forecast-system/access/operational-analysis/initial-conditions-high-resolution/)).

### 3. Methods

To investigate possible pathways through which land surface alterations influence precipitation, we use the diagnostic energy balance (DEB) model for tropical precipitation proposed by Srinivasan (2001). Based on this model, the seasonal mean precipitation ( $P$ ) can be expressed as a function of evaporation from the surface ( $E$ ), the net flux at the top of the atmosphere ( $Q$ ), and total precipitable water ( $P_w$ ) in the atmospheric column, as shown below:

$$P = E + \frac{Q}{\left(\frac{C}{P_w} - 1\right)}. \quad (1)$$

Here,  $C$  is a constant with a dependency on surface pressure and temperature, and the whole term in the

denominator represents a form of moist stability. The constant  $C$ , hereafter termed as stability parameter, is computed for each experiment separately using the values of  $Q$ ,  $E$ , and  $P_w$ . The DEB model is known to represent the mean precipitation at seasonal timescales quite well and is based on the moist static energy budget framework of Neelin and Held (1987). The model assumes that the horizontal gradients of moisture and temperature are weak and that the seasonal mean energy storage on land is negligible. However, in the following discussions,  $Q$  represents the sum of net flux at the top of the atmosphere and net flux into the atmosphere from the land surface, although the contribution from the land surface is minimal. Forest cover differences can modulate the above-mentioned parameters governing precipitation. To quantify the role of each parameter, we perturb equation (1) to obtain

$$\Delta P = \underbrace{\frac{\Delta E}{\text{evaporation}}}_{\text{evaporation}} + \underbrace{\frac{(P_o - E_o) \Delta Q}{Q_o}}_{\text{net energy input}} - \underbrace{\left[ \frac{P_{wo} \Delta C - C_o \Delta P_w}{C_o - P_{wo}} \right]}_{\text{moist stability}} \frac{(P_o - E_o)}{P_{wo}}. \quad (2)$$

Here, the subscript ‘ $o$ ’ denotes a reference state. For the purpose of this study, BSL is chosen to represent the reference state.  $\Delta$  represents the departure from the base state for each variable.

The DEB model assumes that horizontal moisture gradients are insignificant, which may not be appropriate over the northwestern boundary of the monsoon domain. To validate the significance of moisture advection, we incorporate the moisture transport over north-west India in the DEB model by modifying equation (2) as shown below:

$$\Delta P = \Delta E + (P_o - E_o) \frac{\Delta Q}{Q_o} - \left[ \frac{P_{wo} \Delta C - C_o \Delta P_w}{C_o - P_{wo}} \right] \times \frac{(P_o - E_o)}{P_{wo}} + S_m. \quad (3)$$

Here,  $S_m$  is the residue term which accounts for the moisture divergence per unit area over the region  $25^\circ$ – $35^\circ$  N,  $66^\circ$ – $76^\circ$  E, relative to BSL. We will use the terminology DEB Modified (DEBM) for this model.

#### 4. Results

The area covered by tropical rainforest over the region,  $5^\circ$ – $40^\circ$  N,  $65^\circ$ – $98^\circ$  E, for each of the experiments are shown in figure 1(e). EXP 1 and EXP 2 have almost the same amount of forest cover, occupying about half of the Indian domain, while in TRF, the forest cover is approximately twice that of EXP1 or EXP2. In figure 1(f), evaporation rate as a function of forest cover is plotted. The evaporation rate is found to exhibit a more or less linear relationship with the forest-covered area, with TRF displaying the highest and BSL displaying the lowest evaporation rates. Figure 1(g) depicts the total precipitable water ( $P_w$ ) as a function of forest cover. Interestingly, the relationship is not linear, and the largest value of  $P_w$  is observed for EXP2 instead of TRF, signaling the plausible significance of moisture advection. However, the interannual variability associated with  $P_w$  is quite high, especially for TRF. The relationship between precipitation and vegetation also exhibits similar behavior, although precipitation is typically found to increase in the presence of vegetation cover (figure 1(h)). EXP2 records the highest amount of precipitation, while it is the lowest for BSL. Further, TRF exhibits the largest variability for all-India rainfall and its average being less than EXP2 could be influenced by the spatial pattern of the precipitation change. Thus, an increase in vegetation cover, despite increasing the latent heat flux over India, does not guarantee a similar increase in seasonal mean monsoon rainfall. This is in partial agreement with the studies by Shukla and Mintz (1982) and Sud and Smith (1985), who showed that evapotranspiration is inconsequential for July rainfall over India. However, our results suggest that it may not be entirely insignificant for the June–September season.

Based on equation (2), the influence of each parameter on precipitation is plotted in figure 2(a). The increase in precipitation that should have been produced by enhanced evaporation alone is highest for

TRF, followed by EXP2 and EXP1. This is expected since the highest and lowest evaporation rates among the three are observed for TRF and EXP1, respectively. However, the enhancement in precipitation due to evaporation increase alone is partially neutralized by a decrease in precipitation due to changes associated with the stability parameter ( $C$ ). An overall cooling of the surface due to the enhanced latent heat loss in the presence of vegetation might have countered the increase in propensity for moist convection. The smallest decrease in precipitation due to the perturbations associated with the stability parameter is for EXP2. This is quite intriguing since EXP1 exhibits the least evaporation increase relative to BSL. The other terms, net radiation and total precipitable water, make relatively smaller contributions to the changes in precipitation. However, the effect of  $P_w$  is found to be quite significant for EXP2, which is almost of the same order of magnitude as the effect of  $C$ . Figure 2(b) depicts the combined effect of the different parameters on precipitation and a comparison with the CFSv2 simulations. The DEB model estimates the precipitation changes quite accurately, although the values are slightly higher for EXP2. Thus, we show that modifying the vegetation cover impacts precipitation at seasonal time scales primarily through three pathways: changes in evaporation, the net energy input into the atmosphere, and atmospheric stability. Precipitation increase is the highest for EXP2 due to the combined effect of the three parameters, despite the evaporation remaining lower than for TRF.

Figures 3(a)–(c) depicts the spatial map of evaporation anomalies (relative to BSL) due to the introduction of vegetation for TRF, EXP1, and EXP2, respectively. The regions exhibiting evaporation increase coincide almost precisely with the areas of vegetation change. However, the increase is not uniform everywhere, which can be due to variations in local climate and soil type distributions. The spatial pattern of precipitation (figures 3(d)–(f)) bears little resemblance to the spatial pattern of evaporation changes, except between  $20^\circ$  N and  $30^\circ$  N. This agrees with prior discussions on the importance of other parameters. Vegetation changes are found to create an alternating high-low pattern of precipitation over the Indian region in the north-south direction. Precipitation increases in the southern peninsular region while it decreases northward of it till around  $20^\circ$  N. The strongest band of increase is observed between  $20^\circ$  N and  $30^\circ$  N latitudes. This pattern of precipitation change is present in all three experiments but with varying intensity and east-west extent. The increase north of  $20^\circ$  N is the strongest in TRF, with the band extending all the way from the Bay of Bengal coast to the Arabian sea coast. It is also accompanied by the strongest negative precipitation anomalies south of  $20^\circ$  N. Positive precipitation anomalies of a similar kind are observed in EXP2 as well north of  $20^\circ$  N, but

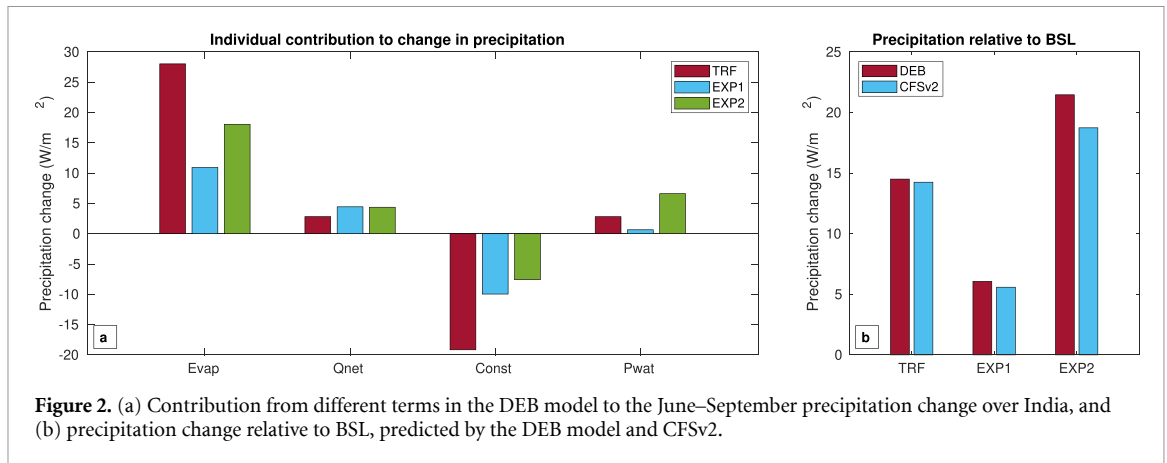


**Figure 2.** (a) Contribution from different terms in the DEB model to the June–September precipitation change over India, and (b) precipitation change relative to BSL, predicted by the DEB model and CFSv2.

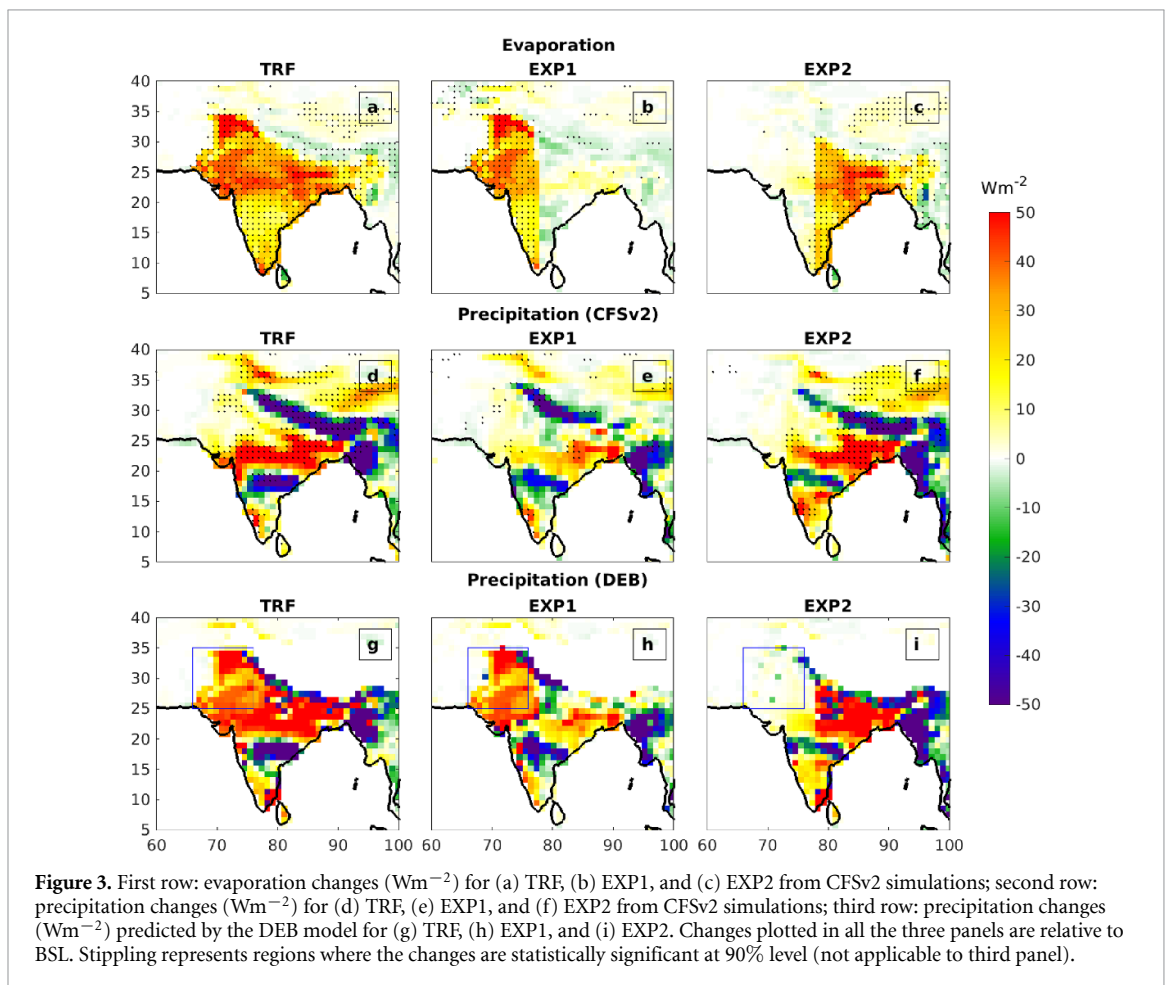
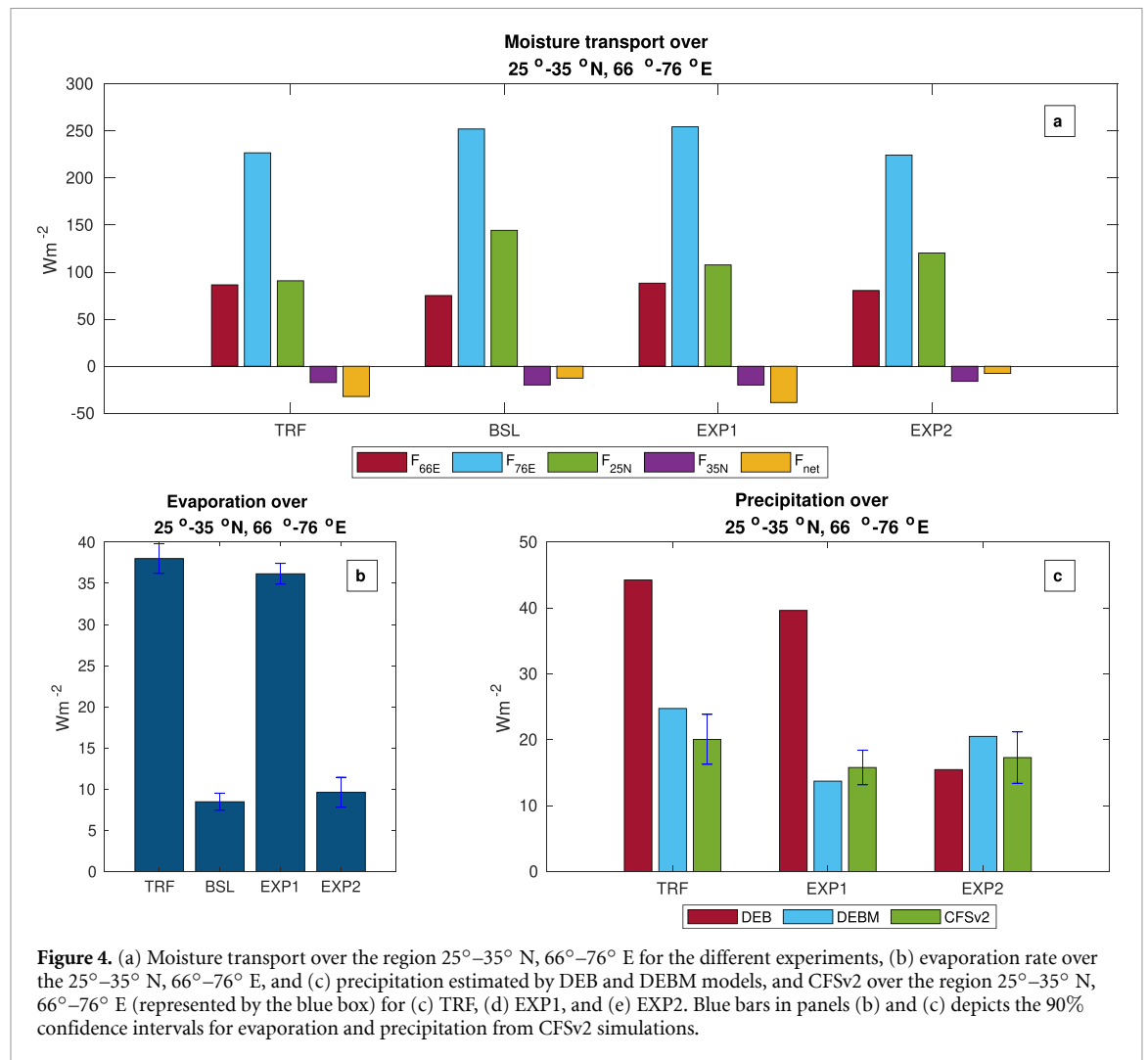


**Figure 3.** First row: evaporation changes ( $\text{Wm}^{-2}$ ) for (a) TRF, (b) EXP1, and (c) EXP2 from CFSv2 simulations; second row: precipitation changes ( $\text{Wm}^{-2}$ ) for (d) TRF, (e) EXP1, and (f) EXP2 from CFSv2 simulations; third row: precipitation changes ( $\text{Wm}^{-2}$ ) predicted by the DEB model for (g) TRF, (h) EXP1, and (i) EXP2. Changes plotted in all the three panels are relative to BSL. Stippling represents regions where the changes are statistically significant at 90% level (not applicable to third panel).

the westward extent of these anomalies is less. Further, precipitation enhancement over the south peninsula is highest for EXP2. In EXP1, the enhancement in precipitation is relatively much smaller compared to either TRF or EXP2. The positive rainfall anomalies observed to the north of 20° N and east of 76° E in TRF are significantly reduced in EXP1. One major observation (based on TRF and EXP1) is that the increase in precipitation over the north-western sector is much less than that expected from the increase in evaporation there. Another notable feature is the

decrease in precipitation on the eastern coast of the Bay of Bengal.

The observed spatially non-uniform response in precipitation could be due to the dominance of different pathways in different regions. The DEB model, described earlier, estimates a uniform increase in precipitation throughout the vegetated region for each case when the effect of evaporation increase alone is considered (supplementary figures 2(a)–(c)). However, the impact of changes in net radiation at the top of the atmosphere is spatially confined to the



regions in the eastern sector on the western coast of the Bay of Bengal (supplementary figures 2(d)–(f)). The large increase in precipitation observed for both TRF and EXP2 in this region can be attributed to the changes associated with radiative effects. The decrease in outgoing longwave radiation is found to dominate the radiation changes over this region. The influence of vegetation through this pathway is relatively negligible for EXP1. Thus it can be hypothesized that the absence of enhanced moisture supply from land in the eastern sector might have prevented the anomalous growth of cloud top heights in EXP1. In all three cases, there is a decline in precipitation associated with stability changes, especially over the eastern coast of the Bay of Bengal (supplementary figures 2(g)–(i)). In addition, for both TRF and EXP2, the observed decline in precipitation south of 20° N is due to the modulation via stability changes. Figures 3(g)–(i) shows the relative change in precipitation owing to the combined effect of the three pathways. Qualitatively, the spatial pattern of the CFSv2 precipitation is well captured by the DEB model for each case, except over northwest India and the south-eastern tip of peninsular India.

The abnormal increase in the precipitation estimated by the DEB model over northwest India is primarily due to the increased evaporation. Since the model has a linear dependency on evaporation, it estimates higher rainfall there. This discrepancy could be associated with the assumptions involved in the model. Figure 4(a) shows the different terms in the moisture advection (details mentioned in supplementary text) over the northwest region (25°–35° N, 66°–76° E), depicted by the blue box in figures 3(g)–(i). There is net moisture advection out of this region in all four experiments. It is also found that in both TRF and EXP1, the net moisture advection almost triples that in BSL or EXP2. To discern this further, we analyze the different components of moisture advection. Eastward moisture flux at 66° E is almost the same in all four experiments. However, eastward moisture flux out of the domain at 76° E is higher for EXP1 and BSL compared to TRF and EXP2, while northward moisture flux at 25° N, is the highest for BSL and lowest for TRF. This large reduction in moisture flux at 25° N in TRF is the primary cause for the reduction in net moisture convergence in TRF relative to BSL. The reduction in moisture flux for EXP1 is

due to the combined effect of large eastward moisture advection at the eastern boundary and reduced moisture influx at the southern boundary. Thus, the enhancement in net moisture divergence could have led to the absence of a large increase in precipitation over this region in TRF and EXP1, even though the evaporation has more than tripled relative to BSL (figure 4(b)).

Figure 4(c) shows the spatially averaged precipitation estimate (over the region  $25^{\circ}$ – $35^{\circ}$  N,  $66^{\circ}$ – $76^{\circ}$  E) by the DEB model, the DEBM model, and CFSv2 for TRF, EXP1, and EXP2. The anomalously high precipitation estimates observed over northwest India in TRF and EXP1 for the DEB model are reduced with the DEBM formulation. This corroborates the significance of moisture advection in northwest India, which is in agreement with the results from previous modeling studies with fully saturated soil in this region (Asharaf *et al* 2012, Agrawal and Chakraborty 2016). Therefore, it can be inferred that the impact of an increase in forest cover is abated due to associated changes in moisture advection. The observed changes in moisture advection could be due to changes in surface winds. See supplementary text for a discussion.

## 5. Summary and discussion

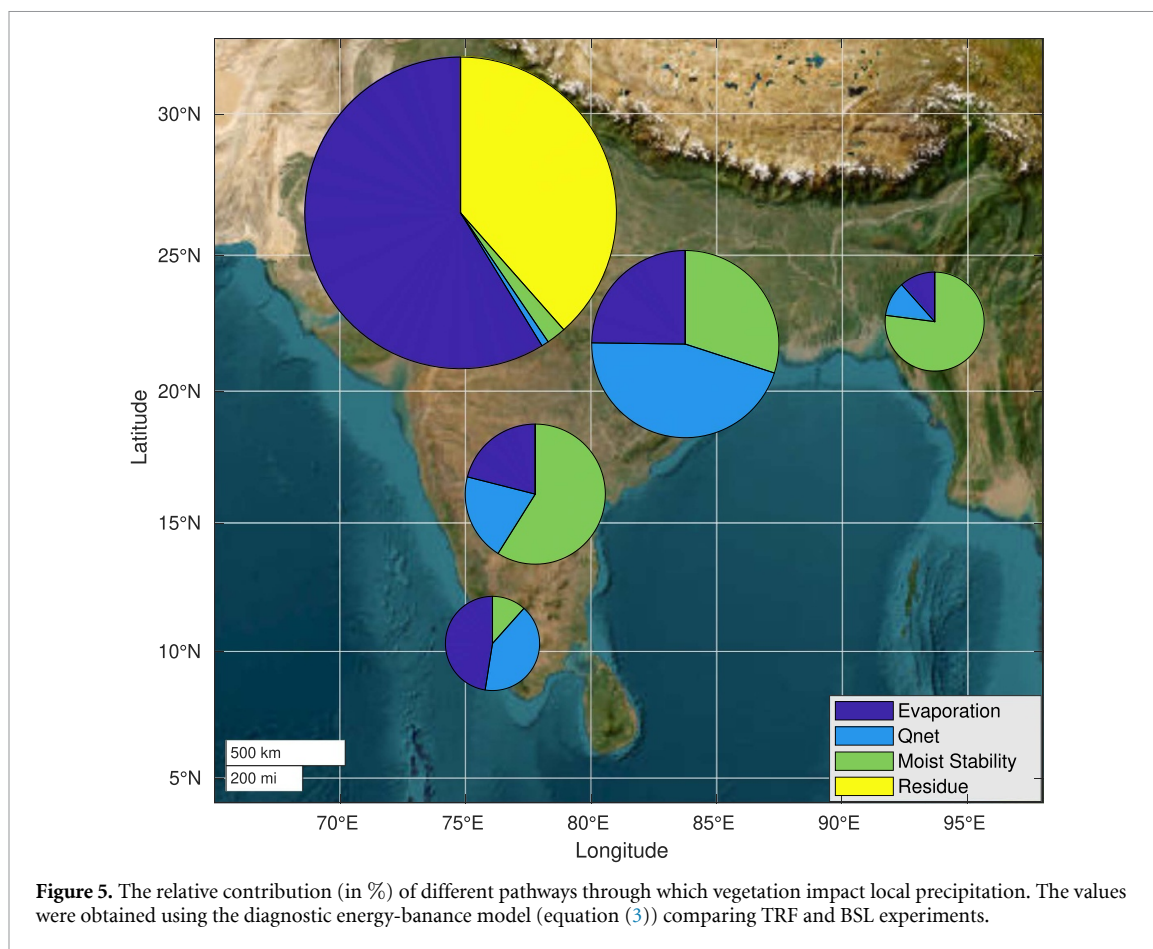
The observed changes in precipitation pattern have two major characteristics. First, in the presence of vegetation, the rain bands appear to have moved northward, which is obvious from the zonal mean precipitation pattern (supplementary figure 4). Enhanced evaporation and an increase in net energy input to the atmosphere at the top of the atmosphere are the major factors driving the northward migration of precipitation. Second, the westward extension of precipitation in the north Indian region depends on the availability of moisture sources over land. The absence of large positive anomalies on the western side in EXP1 and EXP2 provides ample evidence for this. This could be due to the fact that rainfall over these regions is associated with convective systems moving northwestward from the Bay of Bengal (Mooley 1973, Krishnamurti *et al* 1975, Praveen *et al* 2015). In the case of EXP2, these systems are supplemented by the increased moisture supply from vegetation in the eastern region, leading to the enhancement in rainfall. The observed decrease in outgoing longwave radiation in this region is suggestive of this. However, the absence of vegetation westward of  $77^{\circ}$  E prevents any further anomalous moisture supply westward of this, unlike in TRF, for which this augmentation increases precipitation all the way up to the Arabian sea coast. But, a similar increase is absent in EXP1 due to the absence of additional moisture supply from land in the eastern region, which might have quelled the anomalous rain-bearing systems

before reaching the western region. These results are in agreement with past studies that show an intensification of convective activity in a moist atmospheric scenario (Derbyshire *et al* 2004, Baisya *et al* 2018). Therefore, in those regions prone to strong convective rainfall, such as the eastern coast of India, the impact of vegetation changes acting through changes in net energy flux at the top atmosphere is important.

Regions where climatological precipitation is quite low, such as northwest India, experience relatively smaller changes in precipitation for the observed increase in evaporation. Enhanced moisture divergence from these regions, accompanied by a weakened moisture supply from the Arabian sea, is the primary cause. This region is also influenced by the incursion of dry continental air, which suppresses convective activity (Chakraborty *et al* 2002, Bhat 2006, Krishnamurti *et al* 2010) and is also close to the northern limit of the monsoon where a transition from the tropical to midlatitude regime happens. Hence, the role of dynamics cannot be ignored in this region (Hoskins and Karoly 1981, Barlow *et al* 1998), which is also evident from the moisture transport analysis (figure 4). Thus, it can be inferred that regional characteristics of moisture advection and precipitation are instrumental in determining the impact of forest cover. An increase in forest cover over the eastern region is found to have a relatively more substantial impact compared to that over the western region. This supports the hypothesis put forward in the present study that an increase in dryness westward from the Bay of Bengal coast to the Arabian sea coast, similar to that observed in north India, is favorable for all-India-average precipitation due to the combined effect of net energy input increase and moisture availability. The east-west asymmetry in rainfall reported in this study is also supported by the findings of Rodwell and Hoskins (1996) and Chou and Neelin (2003), who have shown that the Rossby wave dynamics, linking the regions of ascent and descent, leads to a westward increase in aridity.

Figure 5 depicts a schematic of the dominant regions of influence of the different pathways. Here, we have not considered the sign of the changes while making this schematic, and the pie charts represent the relative importance of the different mechanisms. Over the northwestern region, the residue term associated with moisture transport is almost as large as the most dominant term, evaporation, while the other two pathways are the least important. This diminishes the influence of evaporation enhancement. Over the eastern coast of the Bay of Bengal and in some regions in peninsular India, the increase in moist stability leads to a decrease in precipitation. Near the western coast of the Bay of Bengal, the increase in precipitation is primarily associated with a modulation via radiative changes, especially





through reduced longwave emission. The importance of cloud radiative effects in the Asian monsoon region has been highlighted in past studies (Rajeevan and Srinivasan 2000, Ramesh and Boos 2022), with the northeastern and northwestern regions in India exhibiting the largest and smallest cloud radiative forcings (Saud *et al* 2016). The relative absence of cloud radiative effects in the northwest could be influenced by this climatology. Over southwest peninsular India, the impact via evaporation and radiative changes together influence precipitation.

Some of the earliest numerical studies on land cover changes and monsoons (Charney 1975, Sud and Smith 1985) have shown that precipitation decreases with increase in deforestation. Our findings agree with their results when precipitation at a nation-wide scale is considered. However, there is considerable spatial heterogeneity in the response and the spatial distribution of vegetation is important. We also find that the pathways through which precipitation is modulated vary regionally.

The pathways recognized in this study are significant from a broader perspective, connecting the regional inhomogeneities to the large-scale atmospheric circulation of which the monsoon is a part. The present study suggests the need to account for geographical variations in the effects that forests have on the local climate. Our findings could also aid in comprehending the changing nature

of land-atmosphere interactions due to human intervention that has reshaped the landscape of India in the last century (Tian *et al* 2014). The methodology can also be employed to understand the impact of various forcings, such as aerosols, greenhouse gases, and the effects of irrigation.

### Data availability statement

The data that support the findings of this study are available upon reasonable request from the authors [10.5281/zenodo.7600227](https://doi.org/10.5281/zenodo.7600227). Data will be available from 30 April 2023.

### Acknowledgments

A C acknowledges the Ministry of Earth Sciences (MoES), Govt of India, for funding this research under the National Monsoon Mission grant. Authors thank Prof. J Srinivasan for the useful comments.

### ORCID iDs

Jerry B Samuel <https://orcid.org/0000-0002-4419-9782>

Arindam Chakraborty <https://orcid.org/0000-0002-4288-0216>

Anagha Paleri <https://orcid.org/0000-0002-6844-8114>

## References

- Adam O, Bischoff T and Schneider T 2016 Seasonal and interannual variations of the energy flux equator and ITCZ. Part II: zonally varying shifts of the ITCZ *J. Clim.* **29** 7281–93
- Agrawal S and Chakraborty A 2016 Role of surface hydrology in determining the seasonal cycle of Indian summer monsoon in a general circulation model *Hydrol. Earth Syst. Sci. Discuss.* **2016** 1–33
- Asharaf S, Dobler A and Ahrens B 2012 Soil moisture precipitation feedback processes in the Indian summer monsoon season *J. Hydrometeorol.* **13** 1461–74
- Baisya H, Pattnaik S, Hazra V, Sisodiya A and Rai D 2018 Ramifications of atmospheric humidity on monsoon depressions over the Indian subcontinent *Sci. Rep.* **8** 9927
- Bamzai A S and Shukla J 1999 Relation between Eurasian snow cover, snow depth and the Indian summer monsoon: an observational study *J. Clim.* **12** 3117–32
- Barlow M, Nigam S and Berbery E H 1998 Evolution of the North American monsoon system *J. Clim.* **11** 2238–57
- Bhat G S 2006 The Indian drought of 2002—a sub-seasonal phenomenon? *Q. J. R. Meteorol. Soc.* **132** 2583–602
- Biasutti M et al 2018 Global energetics and local physics as drivers of past, present and future monsoons *Nat. Geosci.* **11** 392–400
- Bonan G B 2008 Forests and climate change: forcings, feedbacks and the climate benefits of forests *Science* **320** 1444–9
- Boos W R and Korty R L 2016 Regional energy budget control of the intertropical convergence zone and application to mid-Holocene rainfall *Nat. Geosci.* **9** 892–7
- Chakraborty A, Nanjundiah R S and Srinivasan J 2002 Role of Asian and African orography in Indian summer monsoon *Geophys. Res. Lett.* **29** 50-1–50-4
- Chakraborty A, Samuel J B and Paleri A 2023 Role of land surface vegetation in the March of Indian monsoon onset Isochrones in a coupled model *Q. J. R. Meteorol. Soc.* **149** 115–32
- Charney J G 1975 Dynamics of deserts and drought in the Sahel *Q. J. R. Meteorol. Soc.* **101** 193–202
- Chou C and Neelin J D 2003 Mechanisms limiting the northward extent of the northern summer monsoons over North America, Asia and Africa *J. Clim.* **16** 406–25
- Davin E L and Noblet-Ducoudre N D 2010 Climatic impact of global-scale deforestation: radiative versus nonradiative processes *J. Clim.* **23** 97–112
- Derbyshire S H, Beau I, Bechtold P, Grandpeix J-Y, Piriou J-M, Redelsperger J-L and Soares P M M 2004 Sensitivity of moist convection to environmental humidity *Q. J. R. Meteorol. Soc.* **130** 3055–79
- Devaraju N, Bala G and Modak A 2015 Effects of large-scale deforestation on precipitation in the monsoon regions: remote versus local effects *Proc. Natl Acad. Sci. USA* **112** 3257–62
- Donohoe A, Marshall J, Ferreira D and Mcgee D 2013 The relationship between ITCZ location and cross-equatorial atmospheric heat transport: from the seasonal cycle to the last glacial maximum *J. Clim.* **26** 3597–618
- Duveiller G, Hooker J and Cescatti A 2018 The mark of vegetation change on Earth's surface energy balance *Nat. Commun.* **9** 679
- Hoskins B J and Karoly D J 1981 The steady linear response of a spherical atmosphere to thermal and orographic forcing *J. Atmos. Sci.* **38** 1179–96
- Jalilhi C, Srinivasan J and Chakraborty A 2019 Modulation of Indian monsoon by water vapor and cloud feedback over the past 22,000 years *Nat. Commun.* **10** 5701
- Joseph P V, Eischeid J K and Pyle R J 1994 Interannual variability of the onset of the Indian Summer monsoon and its association with atmospheric features, El Nino and sea surface temperature anomalies *J. Clim.* **7** 81–105
- Kang S M, Held I M, Frierson D M W and Zhao M 2008 The response of the ITCZ to extratropical thermal forcing: idealized slab-ocean experiments with a GCM *J. Clim.* **21** 3521–32
- Krishnamurti T N, Kanamitsu M, Godbole R, Chang C-B, Carr F and Chow J H 1975 Study of a monsoon depression (I) synoptic structure *J. Meteorol. Soc. Japan* **53** 227–40
- Krishnamurti T N, Simon A, Thomas A, Mishra A, Sikka D, Niyogi D, Chakraborty A and Li L 2012 Modeling of forecast sensitivity on the March of monsoon Isochrones from Kerala to New Delhi: the first 25 days *J. Atmos. Sci.* **69** 2465–87
- Krishnamurti T N, Thomas A, Simon A and Kumar V 2010 Desert air incursions, an overlooked aspect, for the dry spells of the Indian summer monsoon *J. Atmos. Sci.* **67** 3423–41
- Lee X et al 2011 Observed increase in local cooling effect of deforestation at higher latitudes *Nature* **479** 384–7
- Meehl G A 1994 Influence of the land surface in the Asian summer monsoon: external conditions versus internal feedbacks *J. Clim.* **7** 1033–49
- Mooley D A 1973 Some aspects of Indian monsoon depressions and the associated rainfall *Mon. Weather Rev.* **101** 271–80
- Neelin J D and Held I M 1987 Modeling tropical convergence based on the moist static energy budget *Mon. Weather Rev.* **115** 3–12
- Pathak A, Ghosh S and Kumar P 2014 Precipitation recycling in the Indian subcontinent during summer monsoon *J. Hydrometeorol.* **14** 2050–66
- Paul S, Ghosh S, Oglesby R, Pathak A, Chandrasekharan A and Ramsankaran R 2016 Weakening of Indian summer monsoon rainfall due to changes in land use land cover *Sci. Rep.* **6** 32177
- Praveen V, Sandeep S and Ajayamohan R S 2015 On the relationship between mean monsoon precipitation and low pressure systems in climate model simulations *J. Clim.* **28** 5305–24
- Rajeevan M and Srinivasan J 2000 Net cloud radiative forcing at the top of the atmosphere in the Asian monsoon region *J. Clim.* **13** 650–7
- Rajendran K, Surendran S, Varghese S J and Chakraborty A 2021 Do seasonal forecasts of Indian summer monsoon rainfall show better skill with February initial conditions? *Curr. Sci.* **120** 1863–74
- Ramanathan V, Chung C, Kim D, Bettge T, Buja L, Kiehl J T, Washington W M, Fu Q, Sikka D R and Wild M 2005 Atmospheric brown clouds: impacts on South Asian climate and hydrological cycle *Proc. Natl Acad. Sci. USA* **102** 5326–33
- Ramesh N and Boos W R 2022 The unexpected oceanic peak in energy input to the atmosphere and its consequences for monsoon rainfall *Geophys. Res. Lett.* **49** e2022GL099283
- Rodwell M J and Hoskins B J 1996 Monsoons and the dynamics of deserts *Q. J. R. Meteorol. Soc.* **122** 1385–404
- Saha S K, Halder S, Rao A S and Goswami B N 2012 Modulation of ISOs by land-atmosphere feedback and contribution to the interannual variability of Indian summer monsoon *J. Geophys. Res.* **117** D13101
- Saha S et al 2014 The NCEP climate forecast system version 2 *J. Clim.* **27** 2185–208
- Saud T, Dey S, Das S and Dutta S 2016 A satellite-based 13-year climatology of net cloud radiative forcing over the Indian monsoon region *Atmos. Res.* **182** 76–86
- Schneider T, Bischoff T and Haug G 2014 Migrations and dynamics of the intertropical convergence zone *Nature* **513** 45–53
- Shukla J and Mintz Y 1982 Influence of land-surface evapotranspiration on the Earth's climate *Science* **215** 1498–501
- Srinivasan J 2001 A simple thermodynamic model for seasonal variation of monsoon rainfall *Curr. Sci.* **80** 73–77
- Srinivasan J 2003 Diagnostic study of errors in the simulation of tropical continental precipitation in general circulation models *Ann. Geophys.* **21** 1197–207
- Sud Y C and Smith W E 1985 Influence of local land-surface processes on the Indian monsoon: a numerical study *J. Clim. Appl. Meteorol. Climatol.* **24** 1015–36

- Tian H, Banger K, Bo T and Dadhwal V K 2014 History of land use in India during 1880–2010: large-scale land transformations reconstructed from satellite data and historical archives *Glob. Planet. Change* **121** 78–88
- Wang P X, Wang B, Cheng H, Fasullo J, Guo Z, Kiefer T and Liu Z 2017 The global monsoon across time scales: mechanisms and outstanding issues *Earth-Sci. Rev.* **174** 84–121
- Webster P J 1983 Mechanism of monsoon low frequency variability: surface hydrological effects *J. Atmos. Sci.* **40** 2110–24
- Webster P J, Magana V O, Palmer T N, Shukla J, Tomas R A, Yanai M and Yasunari T 1998 Monsoons: processes, predictability and the prospects for prediction *J. Geophys. Res.* **103** 14451–510
- Zhang B, Tian L, Yang Y and He X 2022 Revegetation does not decrease water yield in the Loess Plateau of China *Geophys. Res. Lett.* **49** e2022GL098025
- Zhang B, Tian L, Zhao X and Wu P 2021 Feedbacks between vegetation restoration and local precipitation over the Loess Plateau in China *Sci. China Earth Sci.* **64** 920–31